Cylindrically anisotropic tubular stalactite with mirror symmetry of displacement under spatially constant body force loading – a finite element model

M. Bednárik, I. Kohút
Geophysical Institute of the Slovak Academy of Sciences[1]

A b s t r a c t : The calcite crystals of the wall of tubular stalactites (soda straws) grow, typically, with their c-axis parallel to the axis of the stalactite. With the direction of the c-axis given, the question is whether the rotation angle with respect to the c-axis is somehow determined, too. Although monocrystalline soda straws have been reported, we will here investigate the properties of hypothetical, but far more interesting, cylindrically anisotropic soda straws.

It will be demonstrated that under the action of spatially constant body force, a cylindrically anisotropic axially symmetric tubular stalactite can, for some special angles of rotation, exhibit mirror symmetry of displacements, typical for isotropic or transversely isotropic tubes.

For various loading modes, we will also address the question of the cylindrically anisotropic configuration optimal with regard to the strain energy.

Key words: calcite, soda straw, cylindrical anisotropy

1. Introduction

The speleothems, especially the worldwide standardized calcite tubular stalactites – soda straws, present some of the few windows into the tectonic and seismic past and shall be dealt with due attention – not only by statistic methods (*Lacave et al., 2002*) or using very rough approximations (*Cadorin et al., 2001*), but taking into account their geometric and structural complexity and individuality of individual specimens. Nowadays, the factor limiting the realism of speleothem stress field modelling, is not

[1] Dúbravská cesta 9, 845 28 Bratislava, Slovak Republic; e-mail: geofmabe@savba.sk

the lack of computing power, but far more the lack of knowledge about the speleothems themselves. The (outer surface) geometry could be measured with 3D laser scanners (*Godin et al., 2002*) or by other means, but the data of inner crystalline structure is simply inaccessible because of the unacceptable invasiveness of our methods. The situation resembles that one in other earth sciences, where the direct access to the studied structures is impossible, too.

What to do in this situation? To think hard about non-invasive methods; to develop the model to the grade that it is prepared for the moment when we are able to feed it with data. And in the meantime, to enjoy the lack of information and speculate as freely as possible.

Therefore, this paper will be quite speculative about how the calcite single crystals of the tubular stalactite may be organized. We will modestly join the common trend of search for "isotropically behaving" anisotropic solids (*He, 2004; Ting, 2005*) by presenting a cylindrically anisotropic speleothem behaving as transversely isotropic.

Our main working tool will be the finite element method. We are well aware of the geometric simplicity of our problem, which could tempt one to try analytical methods and present the exact solutions. For us, however, the way is not our goal and we do not want to obscure simple things by using heavy tools.

2. Elastic constants of calcite single crystal

Let us have the Hooke's law written as $\boldsymbol{\tau} = \mathbf{c}\,\boldsymbol{\varepsilon}$, where

$$\boldsymbol{\varepsilon} = (\varepsilon_{xx}, \varepsilon_{yy}, \varepsilon_{zz}, 2\varepsilon_{yz}, 2\varepsilon_{xz}, 2\varepsilon_{xy})^T \quad \boldsymbol{\tau} = (\tau_{xx}, \tau_{yy}, \tau_{zz}, \tau_{yz}, \tau_{xz}, \tau_{xy})^T \tag{1}$$

are the Voigt 6×1 strain and stress vectors, respectively, and $\mathbf{c}$ is the 6×6 elastic coefficient matrix.

The general form of the elastic coefficient matrix for trigonal crystals can be found e.g. in *Obetková et al. (1990), p. 381*:

$$\mathbf{c} = \begin{pmatrix} c_{11} & c_{12} & c_{13} & c_{14} & 0 & 0 \\ & c_{11} & c_{13} & -c_{14} & 0 & 0 \\ & & c_{33} & 0 & 0 & 0 \\ & & & c_{44} & 0 & 0 \\ & & & & c_{44} & c_{14} \\ & & & & & \frac{c_{11}-c_{12}}{2} \end{pmatrix}, \tag{2}$$

where, as the matrix is symmetric, only the coefficients on and above the diagonal are given.

For calcite, *Chen et al. (2001)*, give the following values of elastic constants (in GPa, in parentheses is the standard deviation in the units of the last digit) – Tab. 1:

Table 1. Elastic constants of calcite (in GPa)

c_{11}	c_{33}	c_{44}	c_{12}	c_{13}	c_{14}
149.4(7)	85.2(18)	34.1(5)	57.9(11)	53.5(9)	−20.0(2)

The constants are given for the axes setting as in Fig. 1.

3. Transformation of elastic constants

An elastic body is cylindrically anisotropic (with respect to the z-axis), if the elastic coefficient matrix $\mathbf{c}^{cyl}$ describing the Hooke's law in cylindrical coordinates is constant throughout the body. As our implementation of finite element method is formulated in Cartesian coordinates, we have to find out, how the elastic constants of the Hooke's law in Cartesian coordinates change from one point of the cylindrically anisotropic body to another.

At point A on the x-axis (Fig. 2), let us have the values of the elastic coefficient matrix $\mathbf{c}(A)$ given with respect to the Cartesian coordinates, as it is usual. In Fig. 2 we can see that unit vectors of the unprimed Cartesian coordinates and cylindrical coordinates at point A are parallel (the unit vector of the z-axis points perpendicularly to the Fig. 2 plane towards the reader), therefore (provided the order of components is canonical in both

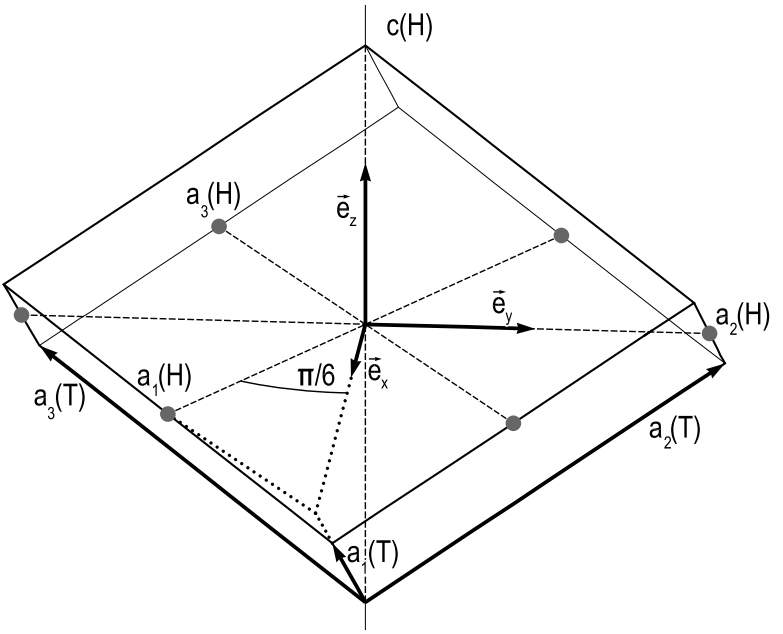

Fig. 1. Cleavage rhomb pseudocell of calcite with trigonal (T), hexagonal (H) and Cartesian axes (after *Chen et al., 2001*).

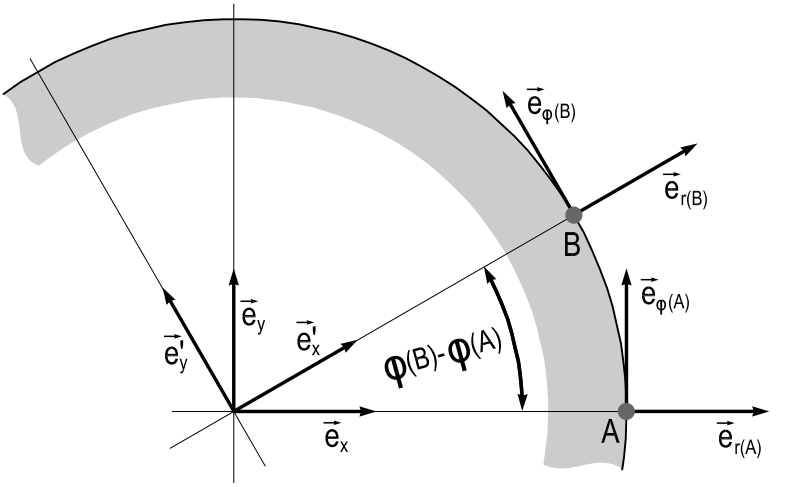

Fig. 2. Relationships between coordinate systems.

coordinate systems, i.e., $x,\ y,\ z$ and $r,\ \varphi,\ z$, respectively) the values of the coefficients in cylindrical coordinates in A are equal to $\mathbf{c}(A)$:

$$\mathbf{c}(A) = \mathbf{c}^{cyl}(A). \tag{3}$$

From the definition of cylindrical anisotropy,

$$\mathbf{c}^{cyl}(A) = \mathbf{c}^{cyl}(B). \tag{4}$$

The rotated (primed) Cartesian unit vectors are parallel with the unit vectors of cylindrical coordinates at point B, therefore

$$\mathbf{c}^{cyl}(B) = \mathbf{c}'(B), \tag{5}$$

where $\mathbf{c}'(B)$ is given with respect to the primed coordinate system. (3) – (5) put together,

$$\mathbf{c}(A) = \mathbf{c}'(B). \tag{6}$$

What we need, however, is $\mathbf{c}(B)$ with respect to unprimed Cartesian coordinates. We transform $\mathbf{c}'(B)$ to $\mathbf{c}(B)$ in the way proposed by *Mehrabadi et al. (1995)*. Their general expressions yield for our simple case of rotation around c-axis (pointing in the direction of z coordinate axis – Fig. 1)

$$\mathbf{c}(B) = \begin{pmatrix} c_{11} & c_{12} & c_{13} & c_{14}\cdot K & c_{14}\cdot L & 0 \\ & c_{11} & c_{13} & -c_{14}\cdot K & c_{14}\cdot M & 0 \\ & & c_{33} & 0 & 0 & 0 \\ & & & c_{44} & 0 & c_{14}\cdot M \\ & & & & c_{44} & c_{14}\cdot K \\ & & & & & \frac{c_{11}-c_{12}}{2} \end{pmatrix}, \tag{7}$$

where $K = (2\cos 2\beta - 1)\cos\beta,\ L = (1 - 4\cos^2\beta)\sin\beta,\ M = (2\cos 2\beta + 1)\sin\beta$. Here, $\beta = \alpha + \varphi$, $\varphi = \varphi(B) - \varphi(A) = \beta - \alpha$, and α is the "initial" rotation angle of the material at point A (Fig. 2). It is important to find out whether the angle in the used transformation formula is the angle by which the piece of continuum is rotated, whereas the coordinate axes stand still, or the opposite – the meaning changes the sign, and misunderstanding can lead to modelling a structure like in Fig. 3. The rightness of the sign

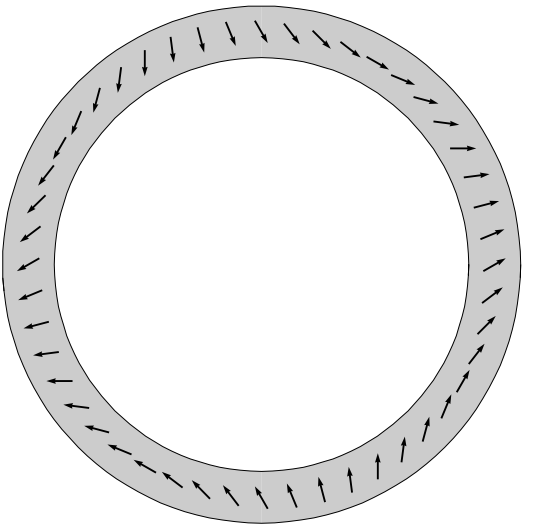

Fig. 3. The soda straw cross-section: structure according to the opposite sign of angle in (7). Arrows indicate the directions of $a_1(H)$ axes.

can be verified by a simple numerical test – the structure (Fig. 5) is and shall behave as axially symmetric, unlike the structure (Fig. 3).

It is very important to have in mind that the matrix of elastic constants (2) is given and the formula (7) is derived for the standard definition of Voigt 6×1 strain and stress vectors (1), while some incompatible definitions can be encountered – mainly where anisotropy is not addressed, e.g. in *Kaiser et al. (1990), p. 200.*

4. Problem formulation

Let us have an axially symmetric, cylindrically anisotropic tubular calcite stalactite of the length L limited by two coaxial cylindrical surfaces – the outer one with radius R_2 and the inner one with radius R_1, attached by its upper end to the planar ceiling of the cave, whereby the ceiling plane and the plane limiting the stalactite from the lower end are perpendicular to its axis. The cave behind the ceiling can be considered as an isotropic halfspace. For

an easier orientation, let us turn the stalactite with the cave upside down and let us introduce Cartesian (having in mind the finite element method will be used to solve the problem) coordinate system (Fig. 4).

For the tubular stalactite only, let us consider the case of cylindrical anisotropy with the matrix of elastic constants independent (in cylindrical coordinates) of r, φ, and z (Fig. 5).

We shall find for which angles of rotation α of single crystals the stalactite will show mirror symmetry of displacement field under action of a spatially constant body force.

5. Cylindrically anisotropic ring – a finite element model

For the purpose of finding the angles of mirror symmetry, it will be just enough to model a stalactite stump with $R_2 = 0.0028$ m, $R_1 = 0.0024$ m,

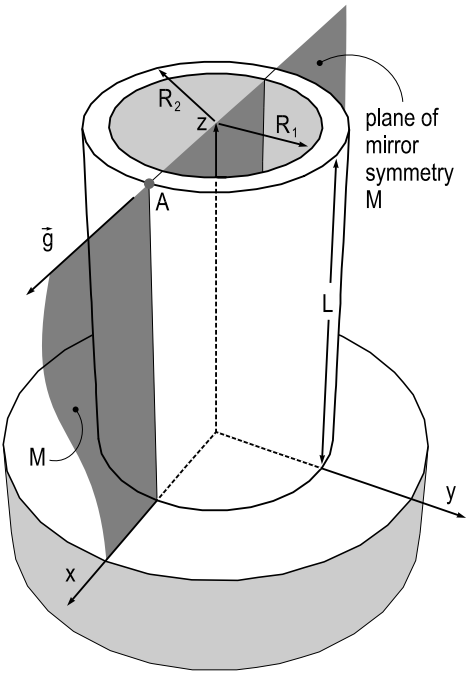

Fig. 4. Tubular stalactite and the axes' setting.

$L = R_2 - R_1 = 0.0004$ m, regularly divided into one layer of 64 hexahedral bilinear finite elements, with their upper base firmly attached (zero displacements prescribed) to the cave ceiling. Let us load the model with spatially constant body force $\rho\vec{g}$, $\vec{g} = (g_x,\ 0,\ 0)$, $g_x = 10\ \mathrm{m\,s^{-2}}$, $\rho = 2712\ \mathrm{kg\,m^{-3}}$.

In Fig. 6, the displacement component u_y at point$A$ as the function of the rotation angle α is shown. For angles where $u_y(A) = 0$, the displacement field is mirror symmetric with respect to the plane M given by $\vec{g}$ and the axis of the tubular stalactite (cf. Fig. 4), as if the soda straw were (transversely) isotropic. As the stalactite is cylindrically symmetric, the computed function $u_y(\alpha)$ is valid for any other direction of $\vec{g}$, provided the coordinate axes are arranged appropriately. Please note the dotted line of $\cos 3\alpha$ (shown only on interval $\langle 0, 5\pi/6\rangle$), enabling us to see that the slopes $|\mathrm{d}u_y/\mathrm{d}\alpha|$ around the roots $\alpha_1 = \frac{\pi}{6} + m\frac{2\,\pi}{3}$, $m \in \{0,\ 1,\ 2\}$ are not equal to the slopes in the vicinity of $\alpha_2 = \frac{\pi}{2} + n\frac{2\,\pi}{3}$, $n \in \{0,\ 1,\ 2\}$, which reflects the different quality of the two sets of roots (to be addressed later).

6. Back to the single crystal

We have seen that there are 6 solutions of our problem on the interval $\langle 0\,,\, 2\,\pi)$. We wonder whether we can provide, on the level of a single crystal, some insight into the number and position of the solution points.

First, let us have a closer look at the strain tensor at point A in the case of mirror symmetry of displacements. As u_y is an odd function of y, $u_y(x,\ 0,\ z) = 0$ everywhere on the plane xz (i.e. M). Therefore, both $u_{y,x}(x_A,\ 0,\ z_A) = 0$ and $u_{y,z}(x_A,\ 0,\ z_A) = 0$. As u_x and u_z are even in y, their $\partial/\partial y$ derivatives must be odd in y, and $u_{x,y}(x_A,\ 0,\ z_A) = 0$, $u_{z,y}(x_A,\ 0,\ z_A) = 0$. Consequently, $\varepsilon_{xy}(A) = \varepsilon_{yx}(A) = (u_{x,y} + u_{y,x})/2 = 0$ and $\varepsilon_{yz}(A) = \varepsilon_{zy}(A) = (u_{y,z} + u_{z,y})/2 = 0$. Thus, the strain tensor will have the form

$$\begin{pmatrix} \varepsilon_{xx} & 0 & \varepsilon_{xz} \\ 0 & \varepsilon_{yy} & 0 \\ \varepsilon_{zx} & 0 & \varepsilon_{zz} \end{pmatrix}, \tag{8}$$

where only ε_{xx}, ε_{yy}, ε_{zz} and $\varepsilon_{xz} = \varepsilon_{zx}$ can be non-zero.

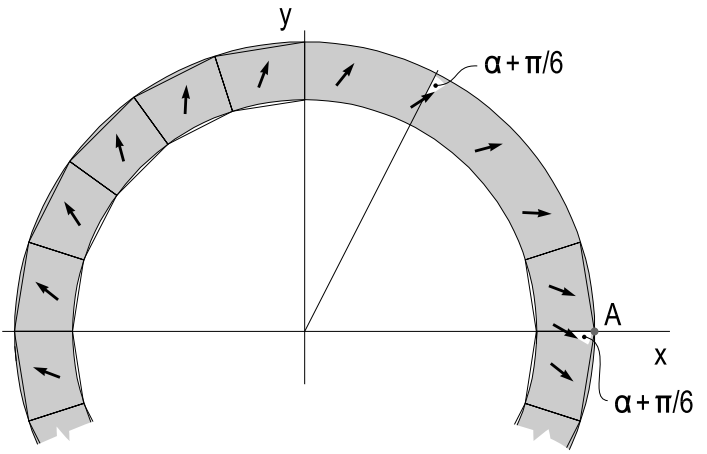

Fig. 5. The soda straw cross-section: cylindrically anisotropic structure. Arrows indicate the directions of $a_1(H)$ axes (c-axes are normal to the section plane). The figure is drawn for the case $\alpha = 0$.

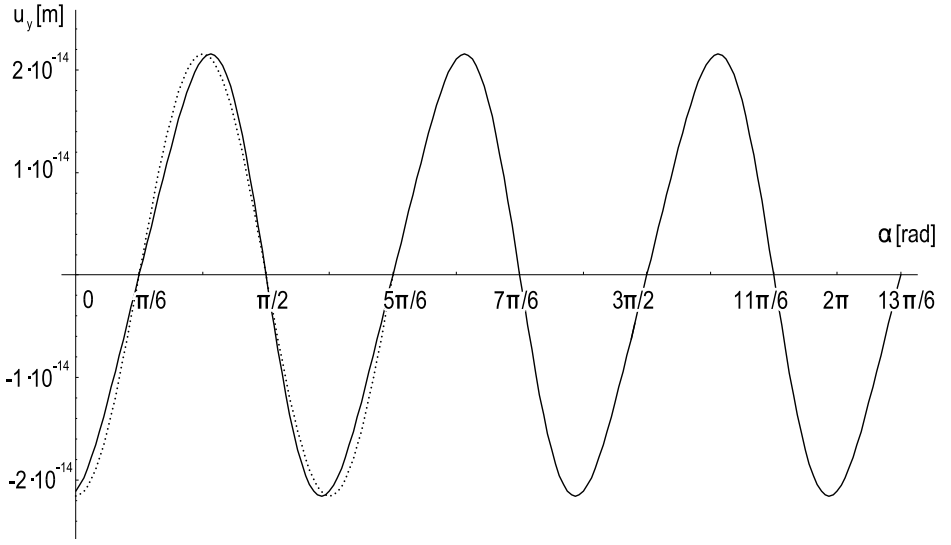

Fig. 6. The displacement $u_y(\alpha)$ at point A (full line) and the function $\cos 3\alpha$ (dotted line).

In the case $\varepsilon_{xz} \neq 0$, eigenvectors of the matrix (8) – principal strain axes – are

$$\begin{aligned} &(0,\ 1,\ 0)\,, \\ &\left(\varepsilon_{xx} - \varepsilon_{zz} - \sqrt{(\varepsilon_{xx} - \varepsilon_{zz})^2 + 4\varepsilon_{xz}^2},\ 0,\ 2\varepsilon_{xz}\right), \text{ and} \\ &\left(\varepsilon_{xx} - \varepsilon_{zz} + \sqrt{(\varepsilon_{xx} - \varepsilon_{zz})^2 + 4\varepsilon_{xz}^2},\ 0,\ 2\varepsilon_{xz}\right). \end{aligned} \tag{9}$$

The case $\varepsilon_{xz} = 0$ is trivial. In both cases (with exception of states when the principal strain directions are undefined), one of the principal strain directions is perpendicular to the plane of mirror symmetry M and the other two lie in it.

Second, let us realize that the displacement field is an outcome of the balance of forces of action – body forces – and of the reaction – the elastic forces. To achieve a mirror symmetric displacement field, with one of its causes – the body force – being spatially constant and thus, mirror symmetric, the other cause – the elastic forces – inevitably must be mirror symmetric, as well. Therefore, the stress tensor at point A will have a similar structure as the strain tensor (8) corresponding to mirror symmetry of displacements – its shearing components, except of τ_{xz} and τ_{zx}, will be zero. Thus, one principal axis of stress is perpendicular to M and identical with one of the principal axes of strain, and the other two coplanar with M, nevertheless, generally not identical with the principal strain axes which lie within M.

The general conditions of strain and stress having (at least) one common principal axis $(0,\ 1,\ 0)$

$$\varepsilon_{xy} = 0, \quad \varepsilon_{yz} = 0, \quad \tau_{xy} = 0, \quad \text{and} \quad \tau_{yz} = 0, \tag{10}$$

yield, for the calcite single crystal rotated by angle α around its c-axis pointing in the direction of z coordinate axis, two equations, which are, as for α, identical:

$$\tau_{xy} = 2\, c_{14} \varepsilon_{xz}\, (-1 + 2\, \cos 2\alpha)\, \cos\alpha = 0, \tag{11a}$$

$$\tau_{yz} = c_{14} (\varepsilon_{xx} - \varepsilon_{yy})\, (-1 + 2\, \cos 2\alpha)\, \cos\alpha = 0. \tag{11b}$$

It can be easily shown that

$$(-1 + 2\cos 2\alpha)\cos\alpha = \cos 3\alpha. \tag{11c}$$

Therefore, all the solutions of (11a, b) on the interval $\langle 0, 2\pi)$ can be expressed as

$$\alpha = \frac{\pi}{6} + k\frac{\pi}{3}, \quad k \in \{0,\ 1,\ 2,\ 3,\ 4,\ 5\}. \tag{12}$$

This set can be split into two subsets:

$$\alpha_1 = \frac{\pi}{6} + m\frac{2\,\pi}{3}, \quad m \in \{0,\ 1,\ 2\}, \tag{13}$$

and

$$\alpha_2 = \frac{\pi}{2} + n\frac{2\,\pi}{3}, \quad n \in \{0,\ 1,\ 2\}. \tag{14}$$

The purpose of this splitting will be clarified in the next section.

7. Energetically optimal cylindrically anisotropic soda straws

We have shown that displacement-mirror-symmetric cylindrically anisotropic calcite soda straws are conceivable. Another question is, whether they can occur in the nature. To address this question, one would need to describe the crystal growth (and, possibly, later recrystallization) process on the tip of the soda straw in very fine details, which, as we have to admit fairly, is beyond our competence.

Therefore, we will rather base our considerations upon the dependence of total strain energy of the ring of crystals (the dimensions are the same as in the section 5) on their angle of rotation α for some loading modes, which come into question as promoters of crystal orientation in the growth phase.

The strain energy of a small-strain deformation of an elastic body can be expressed as

$$E = \frac{1}{2}\int_V \varepsilon_{ij}\,\tau_{ij}\,\mathrm{d}V, \tag{15}$$

where $i,\ j \in \{1,\ 2,\ 3\}$, and 1, 2, 3 stands for $x,\ y,\ z$, accordingly, and the double index summation convention is used. In our model, the integral is approximated by replacing the functions ε_{ij} and τ_{ij} within each element by their central values.

One of the promoters of crystal orientation could be the vertical force of gravity, with $\vec{g} = (0,\ 0,\ g_z)$, $g_z = 10\ \mathrm{m\,s^{-2}}$. The plot of the angle dependence $E_g(\alpha)$ of the strain energy of a cylindrically anisotropic ring loaded only by gravity is shown in Fig. 7. As $u_y(\alpha)$, the $E(\alpha)$ for all presented loading modes is periodic with the period $\frac{2\pi}{3}$. We show only one period of this function on the interval $\left\langle \frac{\pi}{6},\ \frac{5\pi}{6} \right\rangle$ (Fig. 7).

The other possible promoter could be some (a little bit hypothetic) radial body force. To allow for comparison of its effects with those of the gravity, we set its magnitude to the same value as gravity, $g_r = 10\ \mathrm{m\,s^{-2}}$ (Fig. 8). The corresponding angle dependence will be denoted $E_r(\alpha)$.

To complete the list, let us realize that during the (re)crystallization, there could occur tangential forces due to the expansion of growing domains. Let us model this loading mode by an equal division of the ring into 64 larger domains without body forces, alternated by 64 couples of small domains with (almost) opposite body forces (indicated by black arrows in Fig. 9 – the number of elements is smaller for better legibility). The proportions of angular widths of the elements with and without body forces are 1:1:30, respectively.

For this model configuration, it is not easy to find the way the body force should be scaled to gravity to allow the quantitative comparison with other loading modes, so we will show only relative variations of the angle dependence of the strain energy $E_t(\alpha)$ in Fig. 10. An interesting feature are the extra valleys at $\frac{\pi}{2} + n\frac{2\pi}{3}$, $n \in \{0,\ 1,\ 2\}$ and the strain energy maxima attained at "insignificant" angles.

With this exception, the other maxima and minima for these loading modes follow the rule valid for the single crystal: the condition of occurrence of strain energy extrema is the coaxiality of stress and strain tensors (*Norris, 2006; Rovati and Taliercio, 2003a; Rovati and Taliercio, 2003b*). Thus, it is not surprising that the energetically extremal configuration is achieved for the same rotation angles as the angles (12) of partial coaxiality of stress and strain tensors, ergo the angles of displacement mirror symmetry.

Worth noting are the flat lines of $E(\alpha)$ corresponding to the monocrys-

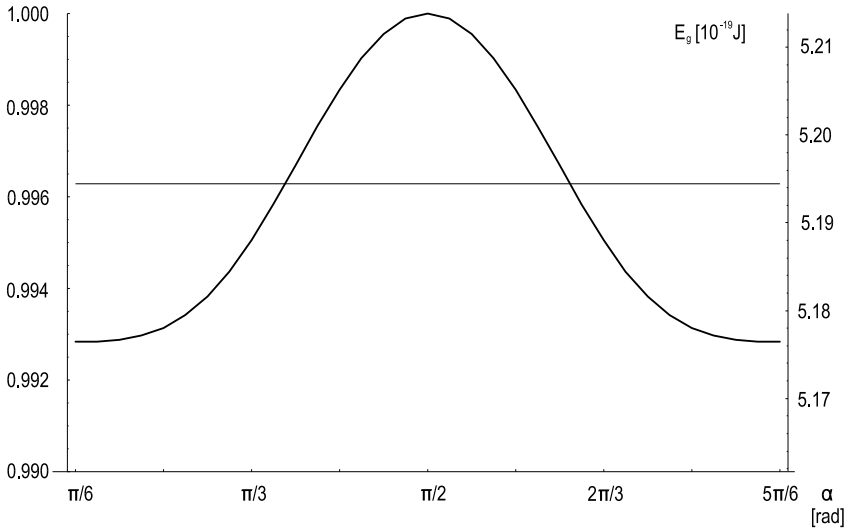

Fig. 7. Angle dependence $E_g(\alpha)$ of the strain energy for vertical gravity loading.

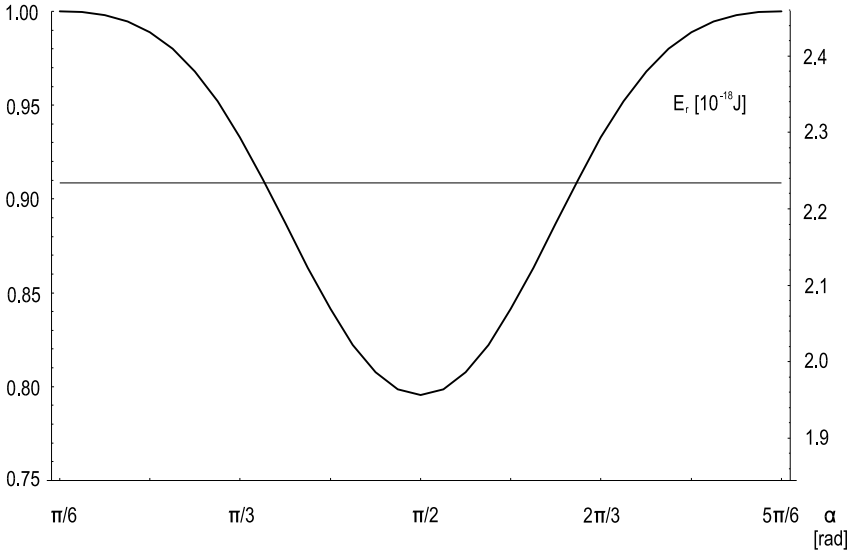

Fig. 8. Angle dependence $E_r(\alpha)$ of the strain energy for radial body force loading.

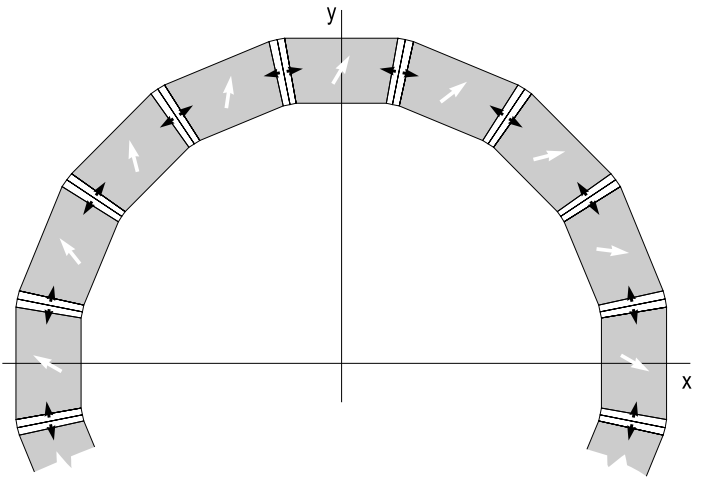

Fig. 9. Cross-section of the model of tangential loading. White arrows indicate the $a_1(H)$ axes of the crystals, black arrows directions of the forces.

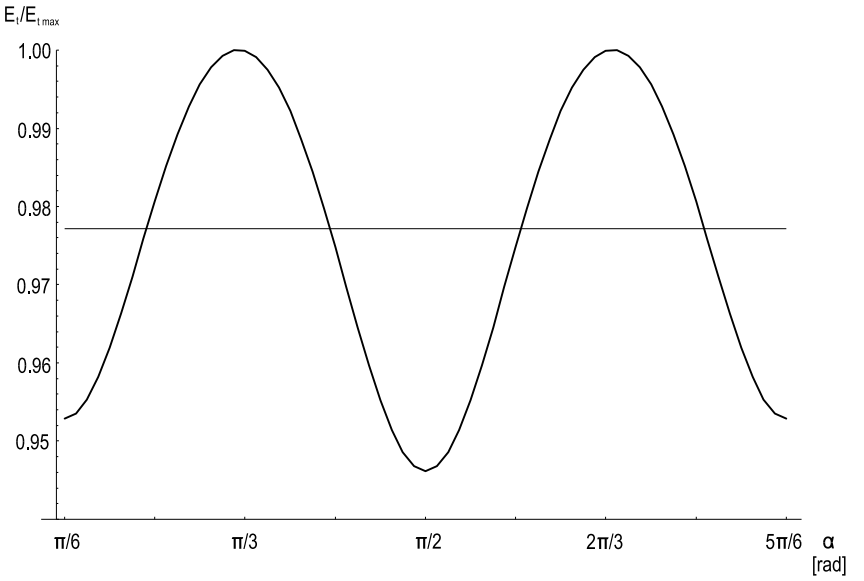

Fig. 10. Angle dependence $E_t(\alpha)$ of the strain energy for tangential loading.

talline soda straw (replace β by α in (7)). Obviously, monocrystalline soda straws are not optimal with regard to the strain energy.

Nevertheless, the relative variations of $E(\alpha)$ in cylindrically anisotropic straws (with the exception of $E_r(\alpha)$) are quite small and thus unlikely to favour an energetically optimal growth over the growth with random angle (resulting to transversal isotropy) or growth dictated by the orientation of one dominant domain (resulting to the whole ring (or even the whole soda straw) being a single crystal).

In the superposition of gravity and radial or tangential body forces, their relative magnitudes are important to judge their importance. Unfortunately, we can well quantify only the gravity – the force with the smallest influence on the orientation (Fig. 7). If the gravity is much bigger than the other two, then these latter forces are insignificant for the orientation of the crystals, in spite of the bigger sensitivity of $E_r(\alpha)$ or $E_t(\alpha)$ alone to α. Interesting is the fact that radial force (independently of its sign) favours angles (14) (Fig. 8), whereas gravity (independently of its sign) favours angles (13) (Fig. 7). With tangential loading, all angles (12) of mirror symmetry are "almost equally" optimal: the small difference between energy levels for angles (13) and (14) – cf. Fig. 10 – probably converges to zero with increasing number of finite elements.

8. Comments and conclusion

As we were dealing with a rather canonical than realistic model of the cylindrically anisotropic tubular stalactite, it made no sense to chase a high computation accuracy by increasing the number of elements or the degree of their shape function. We neither made any error estimates, except of a simple testing of the sensitivity of the results to the number of elements, which brought no bad surprises to us. Thus, we are quite confident that the presented results are good estimates of the orders of magnitudes of the studied quantities. If the orders of displacements and strain energies appear too small to the reader, we make him aware that a ring of calcite with the dimensions given in section 5 weights just $7.1 \cdot 10^{-6}$ kg.

With very simple tools of numerical mathematics, we gained some valuable insights into the problem of tubular stalactite crystalline structure –

the more valuable the harder it is to find a cylindrically anisotropic soda straw in the nature.

Acknowledgments. The authors are grateful to the Slovak Scientific Grant Agency (grants No. 1/3066/06 and 2/6019/26) and APVT grant No. APVT-51-002804 for the partial support of this work.

References

Cadorin J. F., Jongmans D., Plumier A., Camelbeeck T., Delaby S., Quinif Y., 2001: Modelling of speleothems failure in the hotton cave (Belgium). Is the failure earthquake induced? Geologie en mijnbouw, **80**, 3-4, 315–321.

Chen C. C., Lin C. C., Liu L. G., Sinogeikin S. V., Bass J. D., 2001: Elasticity of single-crystal calcite and rhodochrosite by Brillouin spectroscopy. American Mineralogist, **86**, 1525–1529.

Godin G., Beraldin J.-A., Taylor J., Cournoyer L., Rioux M., El-Hakim S. F., Baribeau R., Blais F., Boulanger P., Domey J., Picard M., 2002: Active Optical 3D Imaging for Heritage Applications. IEEE Computer Graphics and Applications, **22**, 5, 24–36.

He Q. C., 2004: Characterization of the anisotropic materials capable of exhibiting an isotropic Young or shear or area modulus. International Journal of Engineering Science, **42**, 19-20, 2107–2118.

Kaiser J., Složka V., Dický J., Jurasov V., 1990: Pružnosť a plasticita I. Alfa, Bratislava 1990, 1st edition, 584 p. (in Slovak).

Lacave C., Egozcue J.-J., Koller M. G., 2002: What can be concluded about seismic history from broken and unbroken speleothems? J. Earthquake Eng., **8**, 3, 431–455.

Mehrabadi M. M., Cowin S. C., Jaric J., 1995: Six-dimensional orthogonal tensor representation of the rotation about an axis in three dimensions. Int. J. Solids Struct., **32**, 3-4, 439–449.

Norris A. N., 2006: Optimal orientation of anisotropic solids. Quarterly Journal of Mechanics and Applied Mathematics, **59**, 1, 29–53.

Obetková V., Mamrillová A., Košinárová A., 1990: Teoretická mechanika. Alfa, Bratislava 1990, 1st edition, 584 p. (in Slovak).

Rovati M., Taliercio A., 2003a: Stationarity of the strain energy density for some classes of anisotropic solids, Int. J. Solids Struct., **40**, 6043–6075.

Rovati M., Taliercio A., 2003b: On coaxiality of stress and strain fields and stationarity of elastic energy in anisotropic solids. Proc. Fifth World Congress of Structural and Multidisciplinary Optimization (WCSMO-5), Lido di Jesolo, Italy, May 19-23, 2003.

Ting T. C. T., 2005: On anisotropic elastic materials for which Young's modulus E(n) is independent of n or the shear modulus G(n,m) is independent of n and m. Journal of Elasticity, **81**, 3, 271–292.